Early Time ICF Capsule Implosion Sensitivities

O. Landen, K. L. Baker, L. Berzak Hopkins, D. S. Clark, B. A. Hammel, D. D. Ho, O. A. Hurricane, J. D. Lindl, E. N. Loomis, L. Masse, C. Mauche, J. L. Milovich, V. N. Goncharov, J. L. Peterson, H. F. Robey, S. A. Yi

January 28, 2016

Disclaimer

This document was prepared as an account of work sponsored by an agency of the United States government. Neither the United States government nor Lawrence Livermore National Security, LLC, nor any of their employees makes any warranty, expressed or implied, or assumes any legal liability or responsibility for the accuracy, completeness, or usefulness of any information, apparatus, product, or process disclosed, or represents that its use would not infringe privately owned rights. Reference herein to any specific commercial product, process, or service by trade name, trademark, manufacturer, or otherwise does not necessarily constitute or imply its endorsement, recommendation, or favoring by the United States government or Lawrence Livermore National Security, LLC. The views and opinions of authors expressed herein do not necessarily state or reflect those of the United States government or Lawrence Livermore National Security, LLC, and shall not be used for advertising or product endorsement purposes.

Indirect-drive ablative Richtmyer Meshkov node scaling

O L Landen[1], K L Baker[1], D S Clark[1], V N Goncharov[2], B A Hammel[1], D D Ho[1], O A Hurricane[1], J D Lindl[1], E N Loomis[3], L Masse[1], C Mauche[1], J L Milovich[1], J L Peterson[1], V A Smalyuk[1], S A Yi[3] and A L Velikovich[4]

[1]Lawrence Livermore National Laboratory, Livermore, CA, USA
[2]Laboratory for Laser Energetics, Rochester, NY, USA
[3]Los Alamos National Laboratory, Los Alamos, NM, USA
[4]Naval Research Laboratory, Washington, DC, USA

landen1@llnl.gov

Abstract. The ablation front Rayleigh Taylor hydroinstability growth dispersion curve for indirect-drive implosions has been shown to be dependent on the Richtmyer Meshkov growth during the first shock transit phase. In this paper, a simplified treatment of the first shock ablative Richtmyer-Meshkov (ARM) growth dispersion curve is used to extract differences in ablation front perturbation growth behavior as function of foot pulse shape and ablator material for comparing the merits of various ICF design options.

1. Introduction

The first indirect-drive ignition designs had a set of computationally derived sensitivities to laser and target (hohlraum and capsule) parameters [1]. As part of developing new designs as warranted by unexpected technological and physics challenges encountered, it is useful to derive approximate analytic models of sensitivities [2] to understand, explain and/or compare simulation-based sensitivities and experimental result trends and scalings between existing and new proposed designs. In this paper, we focus on a simplified analytic model of the early time hydroinstability [3] evolution of perturbations at the capsule surface subject to x-ray drive.

2. Simplified ARM Model

Ignition requires a pulse shape with a low power foot designed (see figure 1) to send a carefully timed series of shocks through the DT shell such that they overtake each other soon after they travel into the enclosed DT gas [4]. This minimizes the in-flight adiabat of the fuel and hence increases its compressibility and the final fuel areal density that can be achieved.
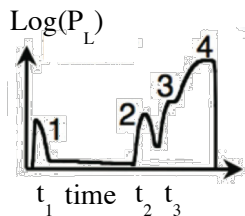

Figure 1. Schematic of laser pulse profile for the example of a 4-shock drive with launch times of shocks identified. The low power section between the first shock picket and 2nd shock launch is denoted the trough.

However, the amplitude of any perturbations of transverse wavenumber k at the capsule surface will begin evolving as a function of k after first shock launch. Extensively evaluated both theoretically and computationally for direct-drive [5,6] where labeled an ablative Richtmyer-Meshkov (RM) instability, the shorter wavelengths even have enough time to oscillate in sign before second shock launch after time $t = t_2 - t_1$. Specifically, the ablation front growth due to the perturbation-rippled shock front [7] that is seeded over an oscillation depth $\approx 1/k$ [8] is reduced and eventually reversed in sign by continuous ablation at a rate V_a. The drive during the picket and trough, by virtue of its long duration compared to the successive shock phases, dominates this ablative RM growth phase. We seek to understand the dependence of the perturbation node k_0 reached at time t_2 on foot pulse shape and ablator material since that largely sets the later acceleration-driven Rayleigh-Taylor (RT) dispersion curve for the case of indirect-drive [9]. In particular, it is advantageous if the node k_0 can be set at $\approx 1/$in-flight shell thickness ΔR, the most potentially damaging ablation front mode based on the combination of RT growth and feedthrough [10].

Noting that for all the indirect-drive ICF foot drive cases of interest shown in Table 1, $k_0 V_a t$ is < 1, so we can approximate the dominant terms in [6,9] as follows:

$$\eta \approx e^{-2kV_a t}\frac{c_s}{\sqrt{V_a V_{bl}}}f(C)sin\left(k\sqrt{V_a V_{bl}}t + 0.3\right) - \frac{c_s}{V_{bl}}g(C)sin\left(1.1\sqrt{C/3}kV_a t + 1\right) \qquad (1)$$

where η is the linear amplitude growth factor, c_s is the postshock sound speed, V_{bl} is the k dependent blow-off velocity $\approx V_a/(2.4kL/\nu)^{1/\nu}$, L is the ablation front width, ν is the thermal conductivity exponent > 1, and C is the first shock compression jump ρ/ρ_0. Conveniently, the arguments $(\sqrt{(C/3)}k_0 V_a t + 1)$ and $(k_0\sqrt{(V_a V_{bl})}t + 0.3)$ cluster around $\pi/2$, so setting the sine terms = 1 and $\eta = 0$ to find the mode number node $\ell_0 = Rk_0$, where R is the average capsule outer radius up to time t_2 (> 95% of R_0), yields:

$$\ell_0 \approx \frac{Rln\left[\left(2.1/(C-1)^{0.9}\right)\left(R\nu/2.4\ell_0 L\right)^{1/2\nu}\right]}{2V_a t} \qquad (2)$$

This is reasonably consistent with the more exact equation (2) in [9] where for the specific case C = 3, $\ell_0 \sim V_a^{-1.5}t^{-0.94}c_s^{0.2}\nu^{-0.1}L^{-.05}$. Ignoring for the moment the weaker log term dependence, equation (2) shows that the node mode number will not depend on capsule scale if the shock merge depth x ~ t is scaled with R. The additional scaling here of interest is with first shock compression, accurate to 5% over relevant C = 2 – 4. We note that as one approaches the incompressible limit (C = 1) corresponding to near zero particle speed behind the shock, there will be little transverse motion and RM growth consistent with simulations [11] and hence no time for phase reversal at any k consistent with equation (2).

3. Model Results

Table 1 lists 8 prior and current implosion designs using either partially Si-doped CH polymer capsules (CH) [3], undoped High Density Carbon (HDC) [12] or partially Cu-doped beryllium (Be) [13]. The drives are designated by the number of shocks, and by adiabat-shaped (AS) [3] in the CH cases where picket and/or trough T_r are modified relative to the regular NIC 4-shock and High-Foot 3-shock designs to create a more strongly decaying first shock [14,15]. Because V_a is typically only 10% of the first shock speed u_s, we can assume the ablation front never reaches the inner mass elements that are either doped or sensing the decaying portion of the first shock. The first shock compression ratios C vs T_r can then be extracted from undoped material shock Hugoniot experiments and simulations of shocked ρ vs pressure P for CH [16], HDC [17] and Be [18] and simulations relating P to picket T_r. The conductivity exponent ν as inferred from code-calculated ablation front density profiles [9] is 1.3 and approximated as the same for all designs since a 30% uncertainty in ν translates to only a 10% (3% per [9]) change in ℓ_0. We note that this value of $\nu = 1.3$ is well below the

radiative diffusion value of 3 because low Z x-ray ablation is only a weakly diffusive process even for NIF timescales. It is also below the electron thermal conduction exponent of $\approx$ 1.5-2 predicted [19] for dense partially ionized low Z plasmas, suggesting volumetric x-ray bleaching is probably dominant.

The key parameter, the ablation rate $V_a = dm/dt/\rho$, is scaled either from simulations for CH [9] or higher T_r planar HDC and Be data [20]. Defining an exhaust velocity v_{ex} and ablator albedo α, we recall that the generalized form of the mass ablation rate $dm/dt \sim T_r^4(1-\alpha)/v_{ex}^2 \sim T_r^4(1-\alpha)/((Z+1)T_e/A)$ and assuming the ablated T_e scales with T_r, $dm/dt \sim T_r^3(1-\alpha)/((Z+1)/A)$. C is not fully ionized at these foot T_r drives, leading to $(1-\alpha_C)$ scaling as $T_r^{-0.3}$ [21]. By contrast, we assume fully ionized Be for a relevant ablated $T_e \approx T_r > 80$ eV [22] and hence a T_r independent lower average albedo ($\approx$15 vs 30%). The specific heat $(Z+1)/A$ of Be is taken to be 4/9, while for CH it is assumed to be between 8/13 and 8.5/13 and for the higher T_r HDC designs, 6.5/12. Combining this information while ensuring consistency with existing data and simulations, V_a becomes $4.4T_r^{2.7}/\rho$, $5.3T_r^{2.7}/\rho$ and $8.0T_r^{3.0}/\rho$ μm/ns with T_r in heV and ρ in g/cc for CH, HDC and Be, respectively. The ordering in mass ablation rate follows from the lower $(Z+1)/A$ of HDC and Be vs CH and the lower albedo of Be [23]. We also assume isentropic decompression at the ablation front $\rho_{trough}/\rho_{shock} = (P_{trough}/P_{picket})^{3/5}$ when the trough $T_r <$ picket T_r in calculating an average V_a. Since $V_a \sim 1/C$, current 4% uncertainties in first shock compression C lead to only a 1-1.5% uncertainty in ℓ_0 through largely cancelling C terms in equation (2). The ablation front widths L are based on CH implosion simulations [9], scaling as $T_r^{1.9}/\rho$. We approximate the multiplicative constant on L as the same between C and Be since the Planck mean free path at relevant 50 < T_r < 100 eV is an average below and above the more absorptive C K edge while it predominantly senses above the less absorptive Be K edge [24]. Moreover, a 30% uncertainty in L only translates to a 5% uncertainty in ℓ_0.

Table 1. Capsule and foot drive design values, calculated first shock RM relevant parameters and calculated first RM node by 2nd shock launch and first RT node mode numbers at peak acceleration.

| Ablator | Design | R | Picket T_r | Trough T_r | C | <L> | <V_a> | t | l_0 | l_0 |
		(μm)	(eV)	(eV)		(μm)	(μm/ns)	(ns)	RM	RT
CH	NIC	1126	63	63	2.4x	0.7	0.5	11.5	116	160
CH	HF	1132	93	85	3.1x	1.2	1.1	7	65	90
HDC	4-Sh	1110	105	105	1.8x	0.7	1	2.5	298	260±15
HDC	3-Sh	1110	123	115	2x	0.9	1.3	2	242	200±15
Be	4-Sh	1051	100	80	2.3x	1	1.6	7.7	62	73
Be	3-Sh	1050	120	103	2.7x	1.3	2.6	5.5	43	28
CH	4-Sh AS	1126	85	63	3x	1	0.8	8	85	75
CH	3-Sh AS	1132	93	70	3.1x	1.1	1	9	63	75

A comparison of the last 2 columns on Table 1 shows that the RM node l_0 analytic scaling from equation (2) quantitatively tracks the calculated RT growth node [3,13,25], confirming the importance of the first shock in setting the hydroinstability dispersion curve. Many of these RT node locations have already been confirmed by RT experiments [15,25]. We caution that we only expect rough one-to-one correspondence between RM and RT modes since simulations and a more accurate analytic model [9] show that the CH node shifts 20-50% to higher mode number between shock breakout and peak acceleration. Nevertheless, we can understand the trends in l_0 relative to the CH 4-shock NIC l_0 as follows: HDC l_0 is substantially greater as the product of $V_a \sim T_r^{2.7}/(C\rho_0)$ and t which is approximately $\sim \Delta R/u_s \sim 1/(\rho_0 u_s) \sim 1/(T_r^{1.4}\sqrt{\rho_0})$ yields $V_a t \sim T_r^{1.3}/(C\rho_0^{1.5})$ which is dominated by the 3.5x larger ρ_0 of HDC. The Be l_0 is less as has $\approx$2x higher mass ablation rate at a given T_r. The CH 3-

shock High-foot and AS l_0 with higher picket and trough T_r are less as $V_a \sim T_r^{2.1}$ (substituting for the CH Hugoniot scaling [16] $C\rho_0 \sim T_r^{0.6}$) increases faster than $t \sim 1/u_s \sim 1/T_r^{1.4}$ decreases. This also explains why all 3-shock designs have lower predicted l_0 than the companion lower T_r 4-shock designs. The 4-shock AS l_0 is less as the larger picket V_a, L and C overcomes a shorter t.

4. Conclusions

We have derived a simple, approximate formula for the first shock driven ablation front dispersion node l_0 of indirect-drive implosions for arbitrary foot pulse shape and ablator material. The scaling explains why the 3-shock CH and all Be ignition designs can provide lower l_0 approaching the RT mode of greatest concern $l \approx R/\Delta R \approx 40$, which also happens to be near the dominant mode seeded at the contact discontinuity of the capsule support thin plastic membranes [26].

References

[1] Haan S et al 2011 *Phys. Plasmas* **18** 051001
[2] Landen O et al 2011 *Phys. Plasmas* **18** 051002
     Lindl J et al 2014 *Phys. Plasmas* **21** 020501
[3] Clark D et al 2014 *Phys. Plasmas* **21** 112705
     Milovich J et al 2015 *Phys. Plasmas* **21** 112702
[4] Munro D et al 2001 *Phys. Plasmas* **8** 2245
[5] Goncharov V 1999 *Phys. Rev. Lett.* **82** 2091
     Velikovich A et al 2000 *Phys. Plasmas* **7** 1662
[6] Goncharov V et al 2006 *Phys. Plasmas* **13** 012702
[7] Loomis E, Braun D, Batha S, Sorce C and Landen O 2011 *Phys. Plasmas* **18** 092702
[8] Aglitskiy Y et al 2002 *Phys. Plasmas* **9** 2264
[9] Peterson J, Clark D, Masse L and Suter L 2014 J *Phys. Plasmas* **21** 092710
[10] Lindl J et al 2004 *Phys. Plasmas* **11** 339
[11] Hammel B et al 2010 *High Energy Density Physics* **6** 171
[12] Mackinnon A et al 2014 *Phys. Plasmas* **21** 056318
[13] Yi S et al 2014 *Phys. Plasmas* **21** 092701
[14] Baker K et al 2015 *Phys. Plasmas* **22** 052702
[15] Macphee A et al 2015 *Phys. Plasmas* **22** 080702
[16] Barrios M et al 2012 *J. Appl. Phys.* **111** 093515
[17] Hicks D et al 2008 *Phys. Rev. B* **78** 174102
[18] Cauble R et al 1998 *Phys. Rev. Lett.* **80** 1248
     Wilson B, Sonnad V, Sterne P and Isaacs W 2006 *J. Quant. Spectrosc. Radiat. Transfer* **99** 658
[19] Lee Y and More R 1984 *Phys. Fluids* **27** 173
[20] Olson R, Rochau G, Landen O and Leeper R 2011 *Phys. Plasmas* **18** 032706
[21] Eidmann K et al 1995 *Phys. Rev. E* **52** 6703
[22] Wilson D et al 1998 *Phys. Plasmas* **5** 1953
[23] Blancard C and Faussurier G 2004 *Phys. Rev. E* **69** 016409
[24] Iglesias C and Rogers F 1993 F *Astrophys. J* **412** 752
[25] Casey D et al 2014 *Phys. Rev. E* **90** 011102
[26] Haan S et al 2013 *Fus. Sci. Tech.* **63** 67
     Nagel S et al 2015 *Phys. Plasmas* **22** 022704